Supplementary Information

Surface Phosphating Activation of $PtMo_6$-Ni-BDC Nanosheets for Enhanced Hydrogen Evolution Reaction

Bo-Cong Shi,[a] Man Jin,[a] Jun-Rui Chen,[b] Pengfei Wu,[c] Dongsheng Geng[a] and Yu-Jia Tang*[a]

[a] School of Chemistry and Materials Science, Nanjing University of Information Science and Technology, Nanjing, 210044, China.

E-mail: tangyujia@nuist.edu.cn

[b] Reading academy, Nanjing University of Information Science and Technology, 219 Ningliu Road, Nanjing, 210044, China

[c] National Key Laboratory for Development and Utilization of Forest Food Resources, Co-Innovation Center for Sustainable Forestry in Southern China, Nanjing Forestry University, Nanjing 210037, China.

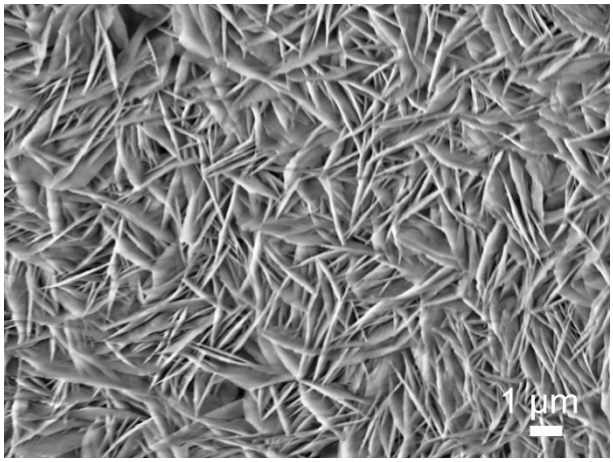

Figure S1. SEM image of Ni-BDC nanosheets grown on NF.

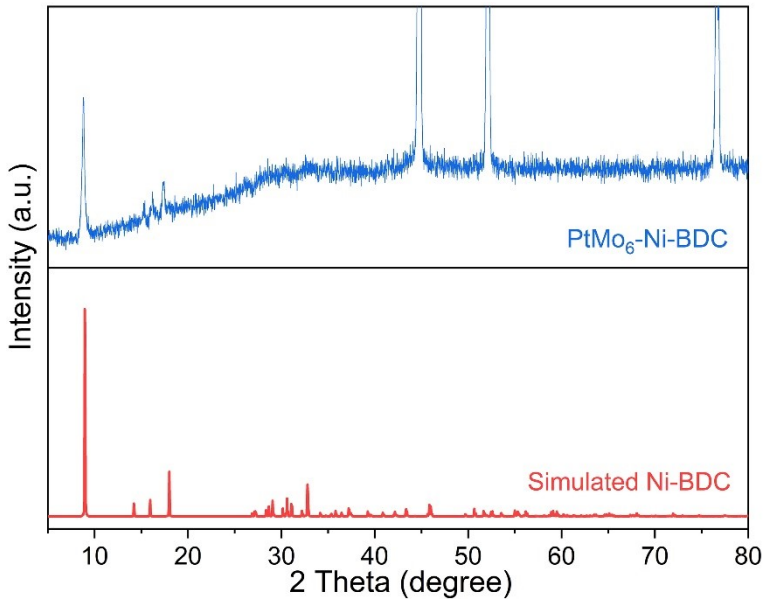

Figure S2. XRD spectra of $PtMo_6$-Ni-BDC on NF and simulated Ni-BDC.

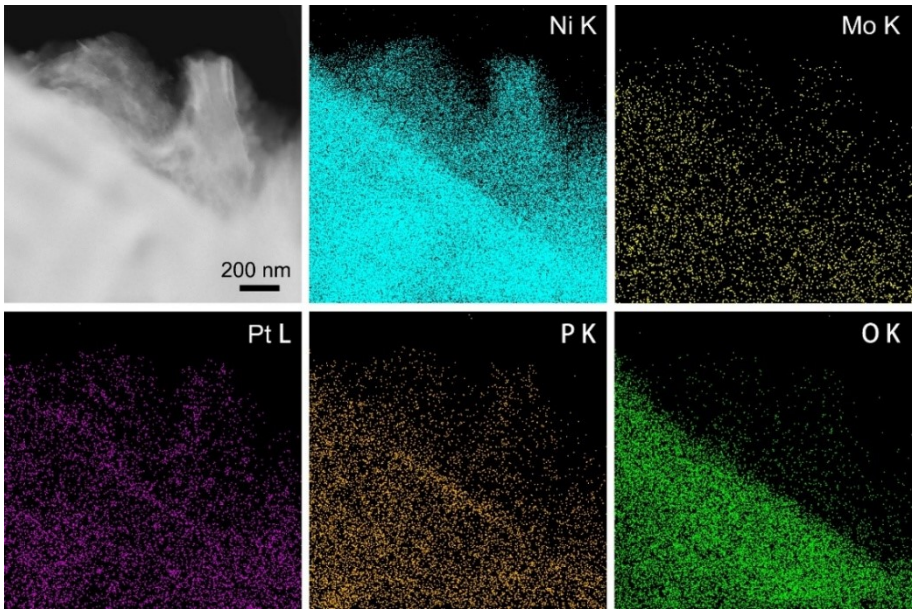

Figure S3. Mapping images of corresponding elements of Ni, Mo, Pt, P, and O of P-$PtMo_6$-Ni-BDC ultrasonicated from NF.

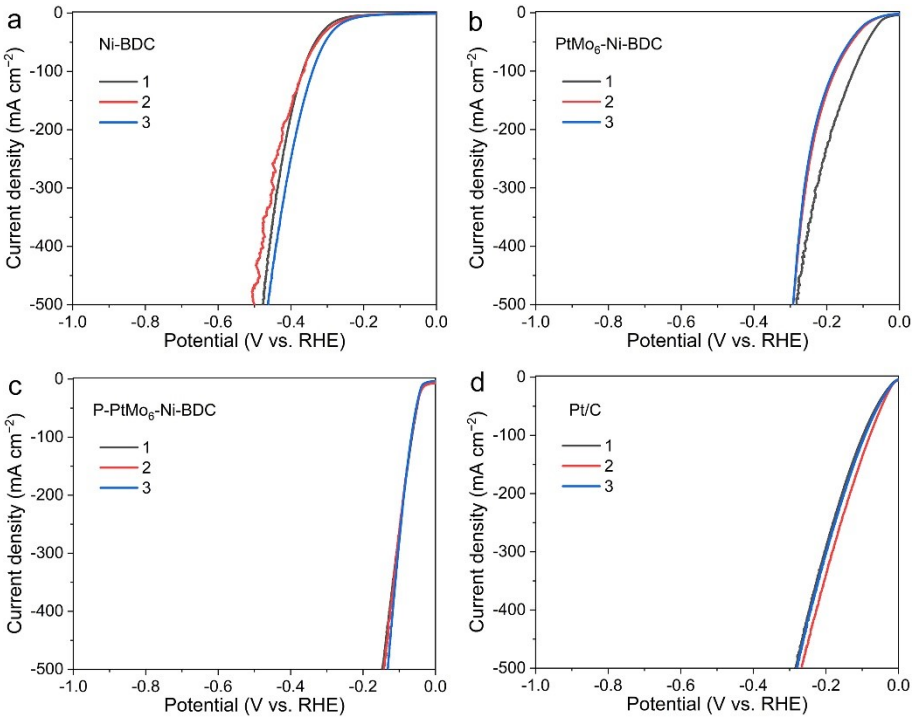

Figure S4. LSV curves of Ni-BDC, $PtMo_6$-Ni-BDC, P-$PtMo_6$-Ni-BDC, and Pt/C on NF measured three times for HER in 1.0 M KOH.

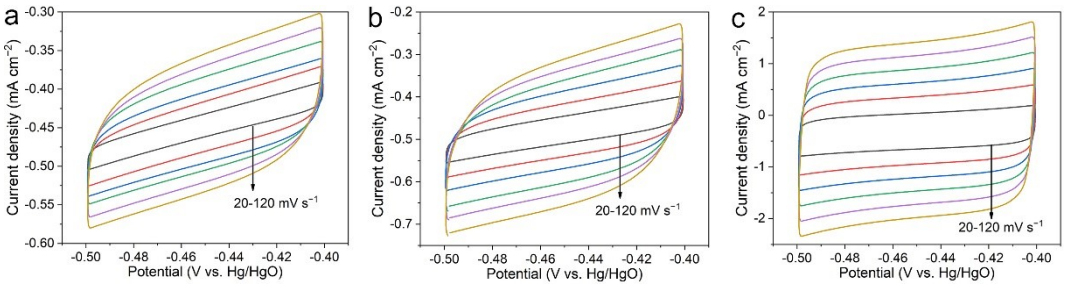

Figure S5. CV curves measured in a non-faradic region of –0.5 to –0.4 V vs. Hg/HgO at different scan rates (20, 40, 60, 80, 100, and 120 mV s^{-1}) in 1.0 M KOH. (a) Ni-BDC, (b) $PtMo_6$-Ni-BDC, and (c) P-$PtMo_6$-Ni-BDC.

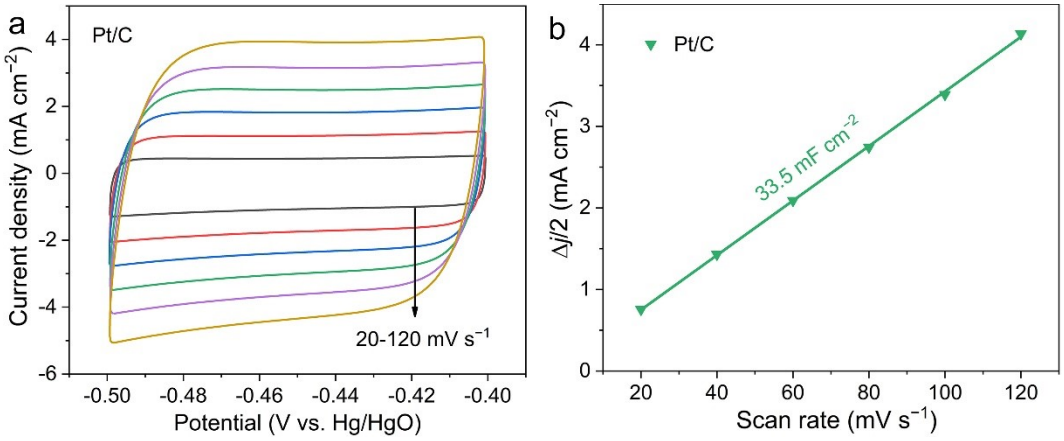

Figure S6. (a) CV curves of Pt/C measured in a non-faradic region of –0.5 to –0.4 V vs. Hg/HgO at different scan rates (20 - 120 mV s^{-1}) in 1.0 M KOH. (b) C_{dl} plot of Pt/C.

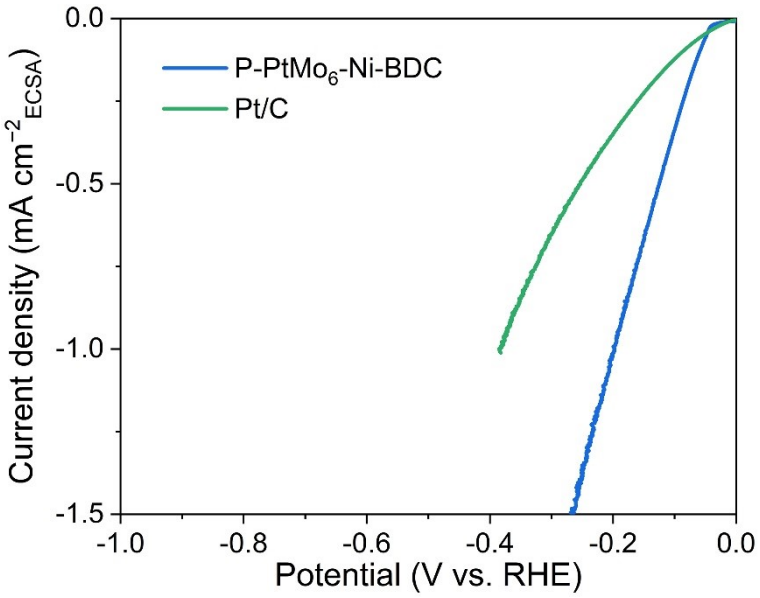

Figure S7. ECSA-normalized LSV curves of P-$PtMo_6$-Ni-BDC and Pt/C for HER.

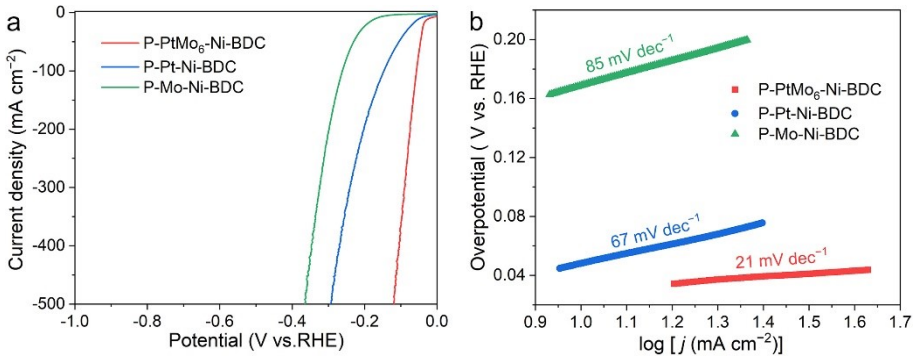

Figure S8. Electrochemical performance of P-$PtMo_6$-Ni-BDC, P-Pt-Ni-BDC, and P-Mo-Ni-BDC prepared by soaking Ni-BDC/NF precursor in solutions of $PtMo_6$, $K_2Pt(OH)_6$, and K_2MoO_4, respectively, for HER measured in 1.0 M KOH. (a) LSV curves and (b) Tafel plots.

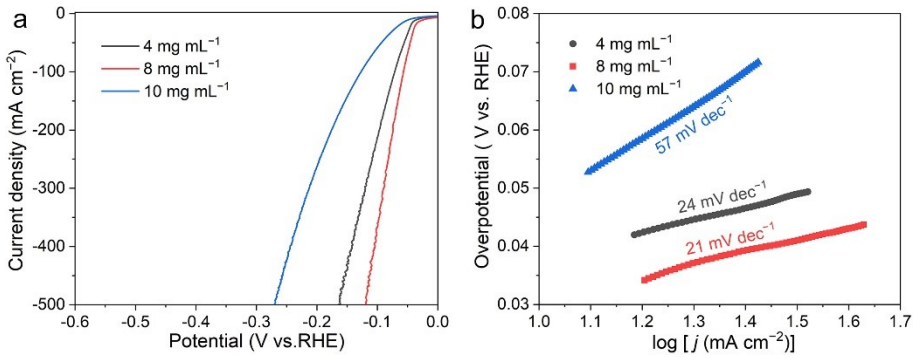

Figure S9. Electrochemical performance of P-$PtMo_6$-Ni-BDC prepared by soaking Ni-BDC/NF precursor in different concentrations of $PtMo_6$ solution (4, 8, and, 10 mg mL^{-1}) for HER measured in 1.0 M KOH. (a) LSV curves and (b) Tafel plots.

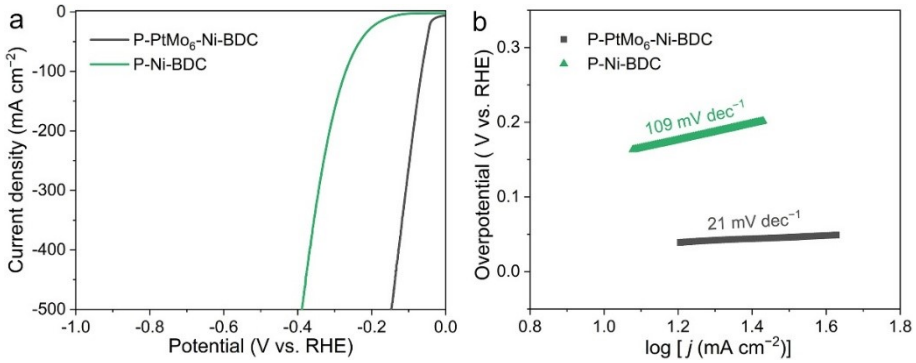

Figure S10. Electrochemical performance of P-$PtMo_6$-Ni-BDC and P-Ni-BDC for HER in 1.0 M KOH. (a) LSV curves and (b) Tafel plots.

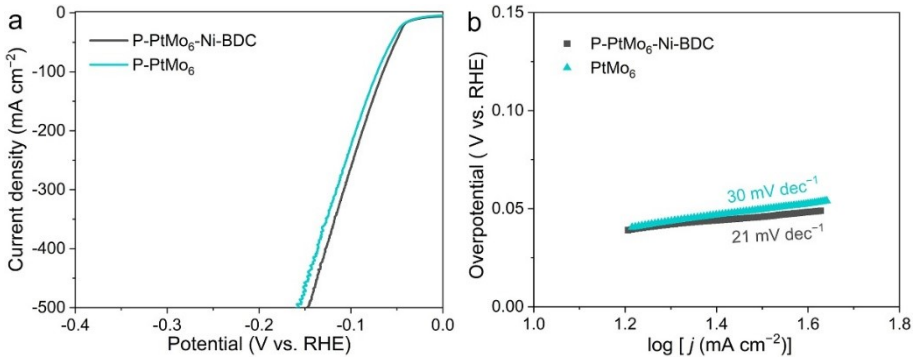

Figure S11. Electrochemical performance of P-$PtMo_6$ and P-$PtMo_6$-Ni-BDC for HER in 1.0 M KOH. (a) LSV curves and (b) Tafel plots.

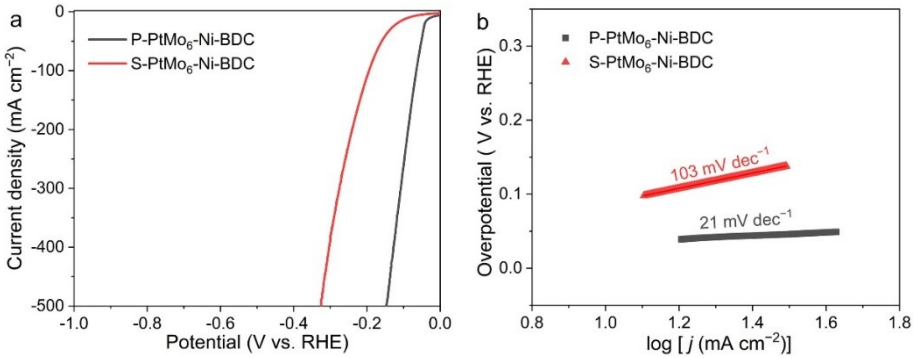

Figure S12. Electrochemical performance of P-$PtMo_6$-Ni-BDC and S-$PtMo_6$-Ni-BDC prepared via phosphidation and sulfidation treatments, respectively. (a) LSV curves and (b) Tafel plots.

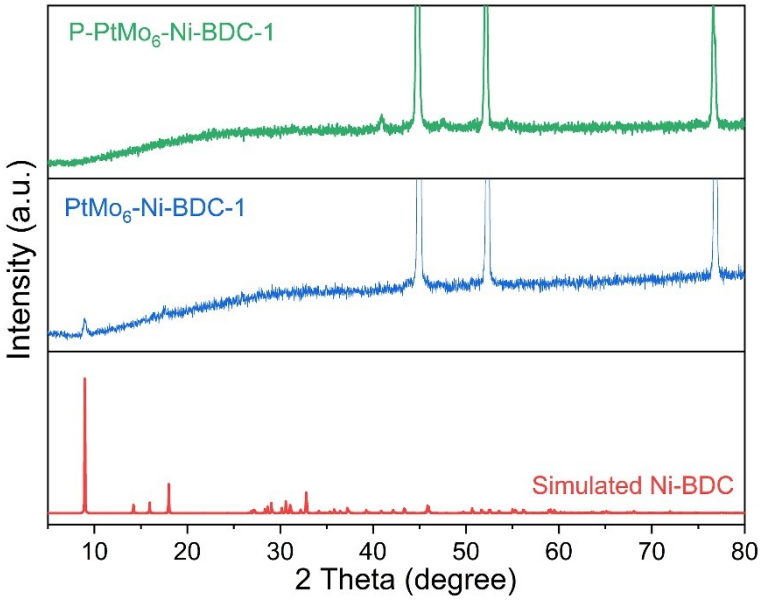

Figure S13. XRD pattern of $PtMo_6$-Ni-BDC-1, P-$PtMo_6$-Ni-BDC-1 on NF, and simulated Ni-BDC.

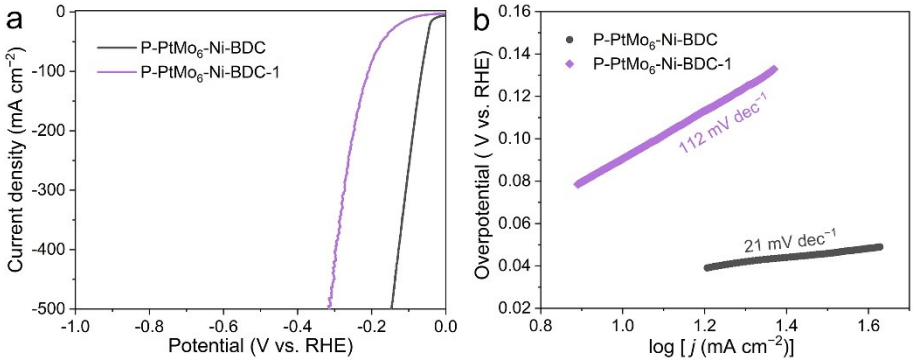

Figure S14. Electrochemical performance of P-$PtMo_6$-Ni-BDC-1 and P-$PtMo_6$-Ni-BDC for HER. (a) LSV curves and (b) Tafel plots.

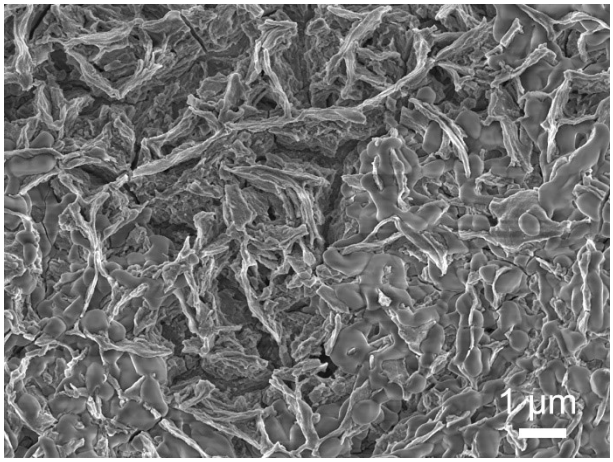

Figure S15. SEM image of P-$PtMo_6$-Ni-BDC on NF after HER.

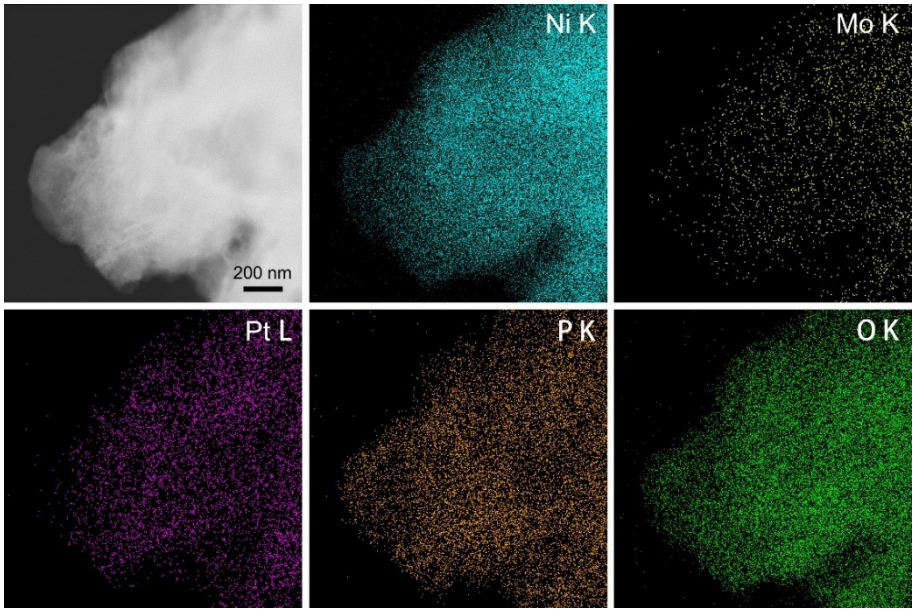

Figure S16. Mapping images of corresponding elements of Ni, Mo, Pt, P, and O of P-$PtMo_6$-Ni-BDC ultrasonicated after HER.

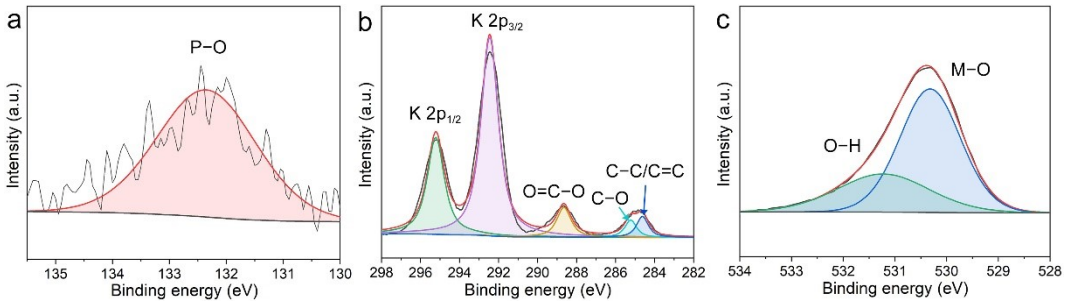

Figure S17. High-resolution XPS spectra of P-PtMo$_6$-Ni-BDC on NF after HER. (a) P 2p, (b) C 1s, and (c) O 1s.

Table S1. Loading mass of P-PtMo$_6$-Ni-BDC on NF. (The area of NF is 8 cm^2)

	Sample 1	Sample 2	Sample 3
Mass of NF (m)	230 mg	234 mg	231 mg
Mass of P-PtMo$_6$-Ni-BDC on NF (n)	256 mg	263 mg	259 mg
Mass of P-PtMo$_6$-Ni-BDC (n-m)	26 mg	29 mg	28 mg
Average loading mass		3.5 mg cm^{-2}	

Table S2. Comparison of HER performance of P-$PtMo_6$-Ni-BDC and recently reported Mo- and Ni-based electrocatalysts in an alkaline medium.

Electrocatalyst	Overpotential at 10 mA cm^{-2} (mV)	Tafel slope (mV dec^{-1})	Substrate	Reference
P-$PtMo_6$-Ni-BDC	**26**	**21**	**Ni foam**	**This work**
Co-Mo-0.125–6N	52	54	Ni foam	[1]
NiCoCu-$Mo_{0.078}$/CF	35	50.12	Cu foam	[2]
Co_3O_4–Mo_2N	100	162.4	Ni foam	[3]
Pt/Ni-Mo-N-O	40.6@100 mA cm^{-2}	49.3	Ni foam	[4]
FeP/Ni_2P/CP	46	50.5	Carbon paper	[5]
MoO_2@Ni_2P	57	61	Carbon paper	[6]
Ni_2P/$MoNiP_2$/MoP-10	20	30.6	Ni foam	[7]
Cu_3P/Ni_2P	88.1	94	Copper foam	[8]
Ni_2P–$Ni_{12}P_5$	76	68.0	Ni foam	[9]
PS-MoNi	30	37	Ni foam	[10]

Table S3. Atomic percentages of corresponding elements of P-$PtMo_6$-Ni-BDC on NF before and after HER according to EDX results.

	before HER	after HER
Ni (at.%)	19.59	61.46
Mo (at.%)	8.71	1.53
Pt (at.%)	1.30	0.79
P (at.%)	10.54	0.82
C (at.%)	30.91	11.92
O (at.%)	38.95	21.35
K (at.%)	/	2.13

Table S4. Concentrations of corresponding elements of P-$PtMo_6$-Ni-BDC ultrasonicated from the NF support before and after HER measured by ICP-MS.

	Before HER	After HER
Ni (mg L^{-1})	30.08	31.57
Mo (mg L^{-1})	13.21	10.07
Pt (mg L^{-1})	4.05	5.64
P (mg L^{-1})	15.89	5.10

References

1 X. Zhang, A. Wu, D. Wang, Y. Jiao, H. Yan, C. Jin, Y. Xie and C. Tian, *Appl. Catal. B-Environ.*, 2023, **328**, 122474.

2 G. Qian, Y. Wang, L. Li, M. Lu, C. Chen, D. Min, Z. Wei and P. Tsiakaras, *Adv. Funct. Mater.*, 2024, **34**, 2404055.

3 T. Wang, P. Wang, W. Zang, X. Li, D. Chen, Z. Kou, S. Mu and J. Wang, *Adv. Funct. Mater.*, 2022, **32**, 2107382.

4 W. Yu, Z. Chen, Y. Fu, W. Xiao, B. Dong, Y. Chai, Z. Wu and L. Wang, *Adv. Funct. Mater.*, 2023, **33**, 2210855.

5 M. Gao, P. Gao, T. Lei, C. Ouyang, X. Wu, A. Wu and Y. Du, *J. Mater. Chem. A*, 2022, **10**, 15569-15579.

6 Z. Zhang, X. Lin, S. Tang, H. Xie and Q. Huang, *J. Colloid Interf. Sci.*, 2023, **630**, 494-501.

7 X. Bu, D. Yin, D. Chen, Q. Quan, Z. Yang, S. Yip, C.-Y. Wong, X. Wang and J. C. Ho, *Small*, 2023, **19**, 2304546.

8 H. Liu, J. Gao, X. Xu, Q. Jia, L. Yang, S. Wang and D. Cao, *Chem. Engin. J.*, 2022, **448**,

137706.

9 Z. Wang, S. Wang, L. Ma, Y. Guo, J. Sun, N. Zhang and R. Jiang, *Small*, 2021, **17**, 2006770.

10 J. Song, Y. Q. Jin, L. Zhang, P. Dong, J. Li, F. Xie, H. Zhang, J. Chen, Y. Jin, H. Meng and X. Sun, *Adv. Energy Mater.*, 2021, **11**, 2003511.